


 Cite this: *Chem. Commun.*, 2025, 61, 19890

 Received 13th October 2025,
 Accepted 14th November 2025

DOI: 10.1039/d5cc05822h

rsc.li/chemcomm

Are the pK_a values of free fatty acids in aqueous solution abnormally high? An NMR and computational perspective

 Themistoklis Venianakis,^a Tjaša Goričan,^b Georgios Papamokos,^a
 Simona Golič Grdadolnik,^b Michael G. Siskos^a and Ioannis P. Gerathanassis^{b,*a}

Accurate dissociation constants of the carboxylic groups of free fatty acids in aqueous solution are unknown, and a wide range of values extending over 5 pK_a units have been suggested. We reinvestigated the problem with the use of 1H and ^{13}C NMR and DFT methods and demonstrate that the pK_a values fall within those of typical organic acids.

Free fatty acids (FFAs) are the main building units of complex lipids, which are a wide group of biological macromolecules with numerous biological properties and an important role in health and nutrition.¹ Short, medium and long chain fatty acids are the digestion products of lipids, which participate in numerous protein-FFA interactions, in the regulation of energy metabolism, and in several inflammation and signaling processes.² FFAs have also been widely used in lipid-based formulations which enhance drug absorption and membrane permeability.³

Free fatty acids due to their hydrophobicity, exist as self-assembled aggregates in aqueous solution which depend on concentration, pH and temperature. Several studies have shown that medium and long chain fatty acids display a broad polymorphism as a function of these parameters. Thus, they display mainly lamellar structures at low pH and/or low temperature and spherical micelles at high pH and/or temperatures and worm-like aggregates in an intermediate regime.⁴ pH controls the ionization state of the carboxylic groups and, thus, the competition between hydrogen bond interactions of the COOH groups and the electrostatic repulsions between the COO⁻ groups.

Several studies have shown that the pK_a values of medium and long chain fatty acids depend on the chain length and values much higher than those for short chain analogues and typical organic carboxylic acids have been reported.^{5a-c} It has been claimed that the pK_a of free fatty acids increases from 6.5 to about 9.0, as

the chain length of the fatty acid increases from C₈ to C₁₆, due to strong ion-dipole interactions of the carboxylate and carboxylic groups. For palmitic (hexadecanoic C16:0) acid the values of 9.7,^{5d} 8.5^{5e} and 8.6–8.8,^{5b} by titration, were reported. For stearic (octadecanoic C18:0) acid, the pK_a values of 9.0^{5f} and 10.15^{5g} were estimated. The pK_a values for elaidic (18:1, *trans*-9), oleic (18:1, *cis*-9), linoleic (18:2, *cis*-9,12) and α -linolenic (18:3, *cis*-9,12,15) acid were found to be 9.95, 9.85, 9.24 and 8.28, respectively.^{5g} It has been suggested that the degree of unsaturation has a significant effect on the pK_a values since it affects the intermolecular distance between the fatty acid molecules due to the significant kinks of the chain. Recent quantum chemical methods reported that the lengthening of the fatty acid chain by one CH₂ fragment leads to an increase in the pK_a by 0.43 units; thus, for stearic acid (C18:0), a surface $pK_a = 10.05$ was calculated,^{5h} in very good agreement with one of the experimental values ($pK_a = 10.15$).^{5h}

From the above, it is evident that large uncertainties exist in the literature regarding the pK_a of short, medium and long-chain fatty acids. The precise estimation of the pK_a values of the free fatty acids (FFAs), however, is of primary importance in protein-ligand interactions since the ionization state of the carboxylic group plays a significant role in complexes with serum albumin,^{6a-g} retinoid X receptor in the mouse brain^{6h} and human brain FA binding protein.⁶ⁱ

The continuing disagreement over the pK_a values of medium and long-chain FFAs and the increasing use of high values in the chemical literature led us to investigate whether the pK_a values of free fatty acids in aqueous solution are abnormally high with the combined use of NMR and DFT methods. 1H and ^{13}C NMR is a rapid and sensitive technique, which allows direct observation of the carboxylic groups undergoing deprotonation.

For caproleic acid, 9-decenoic acid (H₂C=CH(CH₂)₇COOH), NMR experiments were performed at concentrations $c = 2$ mM and 150 mM, which are below and above the critical micelle concentration, respectively. Fig. S1A(a) (SI) presents the 1H NMR spectrum of 150 mM caproleic acid at pD = 9.3. The spectrum remains essentially the same for a period of over 10 days (SI: Fig. S1A(b)).

^a Section of Organic Chemistry and Biochemistry, Department of Chemistry, University of Ioannina, Ioannina, GR 45110, Greece. E-mail: igeroth@uoi.gr

^b National Institute of Chemistry, Laboratory for Molecular Structural Dynamics, Theory Department, Hajdrihova 19, SI-1000, Ljubljana, Slovenia



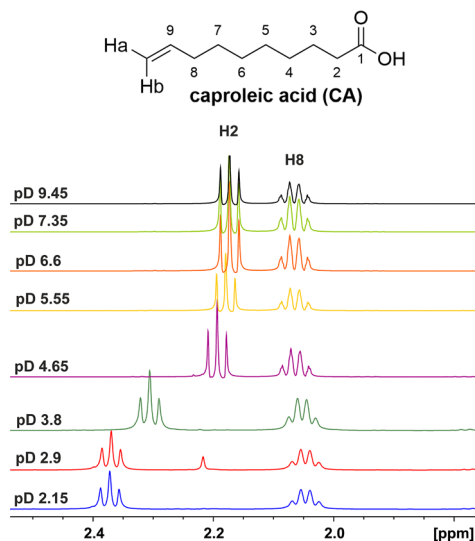


Fig. 1 Aliphatic region of the ^1H NMR spectra (500 MHz) of 150 mM caproic acid in D_2O at various pD values (number of scans = 16, $T = 298$ K). Experimental time of each NMR spectrum is 2 min.

For pD values 10 to 6, the CH_2COO protons do not show any inflection point. At pD < 6 the ^1H NMR spectra are more complex. Thus, at pD = 1.9, the H2, H3, H8 and H10a,b resonances show the presence of two species (SI: Fig. S1B(b)). A non-linear regression analysis of the experimental δ_{obs} of the major species, vs. pD values resulted in the $\text{p}K_{\text{a}} = 4.30 \pm 0.05$ (SI: Table S1). On standing of the solution for approximately one week, the major aggregate with the $\alpha\text{-CH}_2$ protons at $\delta_{\text{obs}} = 2.26$ ppm was transformed to the second one at $\delta_{\text{obs}} = 2.37$ ppm. The chemical shifts of the new major species as a function of pD, are shown in Fig. 1 and resulted in a $\text{p}K_{\text{a}}$ value identical to the previous one. The $\text{p}K_{\text{a}}$ value of both species (SI: Fig. S2 and Table S1) is not significantly different from that for concentrations below the critical micelle concentration ($\text{p}K_{\text{a}} = 3.79$, SI: Table S1). This value is within the expected range of typical organic carboxylic acids, and it is significantly lower than those reported in the literature for free fatty acids with ten carbon chains.

The ionization state of the carboxylic group was further confirmed with $^1\text{H}\text{-}^{13}\text{C}$ HSQC and HMBC experiments. The ^{13}C chemical shifts of the $\alpha\text{-CH}_2$ carbon are essentially the same at pD > 6.5 ($\delta = 40.2$ ppm), which demonstrates that there is no inflection point in this pD range (Fig. 2A). At the low pD = 2.15 (Fig. 2B), the ^{13}C chemical shift ($\delta_{\text{obs}} = 36.7$ ppm) shows a shielding by 3.5 ppm, which is in excellent agreement with values of aliphatic carboxylic acids (3.5 ppm and 3.9 ppm for propionic and valeric acid, respectively).⁷ Similarly, the ^{13}C shift of the COOH carbon ($\delta_{\text{obs}} = 182.6$ ppm) shows a deshielding upon deprotonation ($\delta_{\text{obs}} = 187.1$ ppm) by 4.6 ppm, which is in excellent agreement with the value of 4.7 ppm for propionic and valeric acid.⁷ It is of interest that the two self-assembled aggregated species at pD = 2.15 show identical ^{13}C chemical shifts of the $\alpha\text{-CH}_2$ ($\delta_{\text{obs}} = 36.7$ ppm, Fig. 2B) and carboxylic carbons ($\delta_{\text{obs}} = 182.6$ ppm, SI: Fig. S3), which demonstrates non-ionic COOH groups.

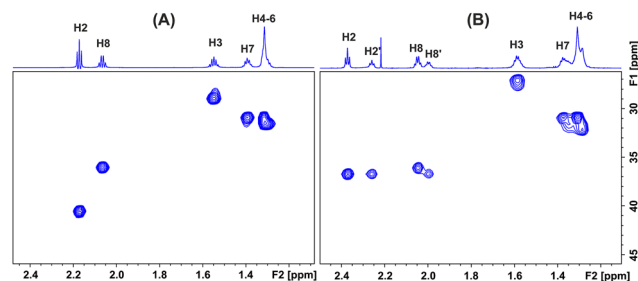


Fig. 2 $^1\text{H}\text{-}^{13}\text{C}$ HSQC NMR spectra (800 MHz) of 150 mM caproic acid in D_2O at: (A) pD 9.45 and (B) pD 2.15 (number of scans = 4, number of increments = 256, $T = 298$ K). Experimental time is 29 min.

The 2D NOESY of caproic acid at pD = 9.45 shows NOEs, which are anti-phase with respect to the diagonal (Fig. 3A); thus, the effective molecular weight of the self-aggregated species is within the extreme narrowing condition. Even with a long mixing time of 800 ms, no NOE cross-peaks were observed between the $\text{CH}_2\text{-COO}^-$ and terminal $\text{C}(10)\text{HaHb}/\text{C}(8)\text{H}_2$, which shows that the parallel arrangement of the ionic aggregated molecules is the most stable structural motif. At pD = 2.15, strong exchange cross-peaks between the two self-assembled aggregated species were observed (Fig. 3B). Again, NOE cross-peaks between the $\text{CH}_2\text{-COOH}$ and terminal $\text{C}(10)\text{HaHb}/\text{C}(8)\text{H}_2$ were not observed, which confirms that the parallel arrangement of the non-ionic aggregated species is the most stable structural motif. It is of interest that the magnitudes of the NOE cross-connectivities between the H2 and H3 protons are different for the two aggregated species, presumably due to different effective molecular weights. This was verified with the use of DOSY experiments.

The DOSY experiment of caproic acid at pD = 9.45 showed the presence of a unique self-aggregated species with diffusion constant $D = 2.06 \times 10^{-9} \text{ m}^2 \text{ s}^{-1}$ (Fig. 4A). At pD = 2.10, the two self-aggregated species with $\alpha\text{-CH}_2$ resonances at $\delta_{\text{obs}} = 2.37$ and 2.27 ppm showed significantly different diffusion constants with $D = 5.2 \times 10^{-10} \text{ m}^2 \text{ s}^{-1}$ and $4 \times 10^{-12} \text{ m}^2 \text{ s}^{-1}$, respectively (Fig. 4B). Since both aggregated species show NOEs in the extreme narrowing condition (Fig. 3), it is evident that they exhibit significant backbone internal motions, despite the extremely slow diffusion mobility of the species with $\alpha\text{-CH}_2$ at $\delta_{\text{obs}} = 2.27$ ppm.

NMR experiments for oleic acid were performed at a concentration of $c = 2$ mM, which is above the critical micelle

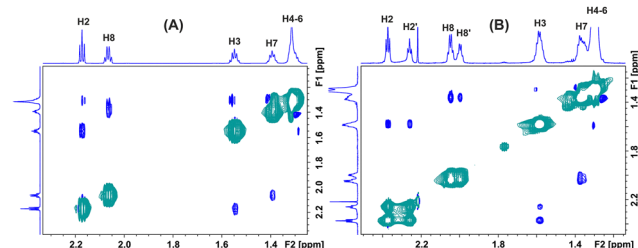


Fig. 3 $^1\text{H}\text{-}^1\text{H}$ NOESY NMR spectra (800 MHz) of 150 mM caproic acid in D_2O at: (A) pD 9.45 and (B) pD 2.15 (number of scans = 32, number of increments = 256, relaxation delay = 1.5 s, mixing time = 0.8 s, $T = 298$ K). Experimental time is 5 h, 50 min.



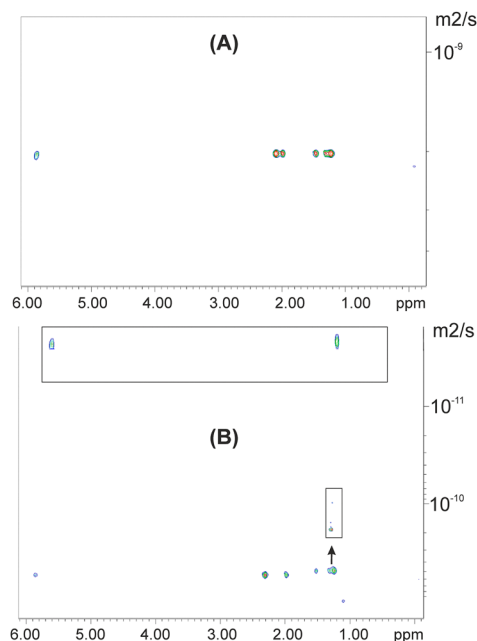


Fig. 4 DOSY experiments of caproleic acid (150 mM in D₂O) at: (A) pD = 9.45 and (B) pD = 2.15. Experimental time is 1 h, 40 min.

concentration. Fig. 5 shows the ¹H NMR chemical shifts of the α-CH₂ group of oleic acid at different pD values. At intermediate pD values < 6.5 different self-aggregated components were observed, which are slow on the NMR time scale. A well-defined titration curve with pK_a = 3.95 (SI: Table S1) was observed, contrary to the literature value of pK_a = 9.85.^{5g} 2D ¹H-¹³C HSQC experiments at pD ≥ 6.5 showed identical chemical shifts of the α-CH₂ carbon (δ_{obs} = 40.6 ppm, SI: Fig. S4), which demonstrates the presence of the carboxylate group without any inflection point in this region. The 2D NOESY spectrum of oleic acid at pD = 10.9 shows that the NOEs are in-phase with respect to the diagonal (Fig. 6A), contrary to the case of caproleic acid. This demonstrates that the self-aggregated species are outside the extreme narrowing conditions. Of particular interest are the long-range NOE cross-connectivities between the H2 and H3 protons with the terminal CH₃ group; this demonstrates that the *cis*-9 double bond induces a

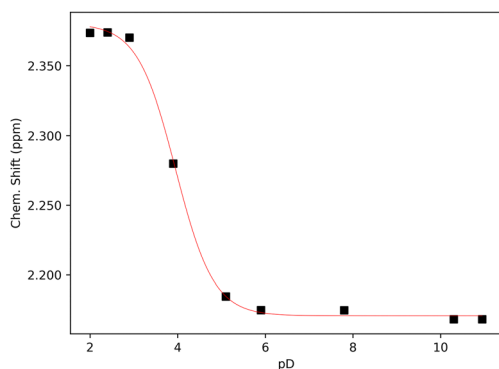


Fig. 5 pD dependence of the α-CH₂ protons of oleic acid (2 mM in D₂O). Experimental time for each NMR spectrum is 32 min.

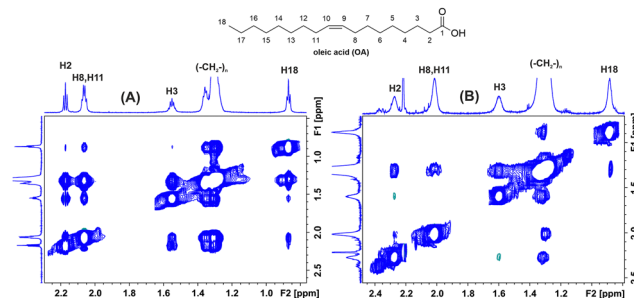


Fig. 6 ¹H-¹H NOESY NMR spectra (800 MHz) of 2 mM oleic acid in D₂O at: (A) pD = 10.9 and (B) pD = 2.1 (number of scans = 64, number of increments = 256, relaxation delay = 1.5 s, mixing time = 400 ms, T = 298 K). Experimental time is 10 h, 40 min.

significant folding of the (CH₂)_n chains and, thus, through-space inter-molecular proximity of the H2 and H3 protons with the terminal CH₃ group (see also the DFT calculations).

At pD = 2.15 the ¹H NMR resonances become significantly broader than those at pD = 10.9 which is an indication of a larger MW of the self-aggregated species. The 2D ¹H-¹³C HSQC experiment showed the non-ionic state of the carboxylic group (δ_{obs} = 36.7 ppm, SI: Fig. S4). The 2D NOESY spectra with mixing times 200, 400 and 800 ms did not show a long-range connectivity between the H2 and H3 protons with the terminal CH₃ group, which demonstrates a different conformational state than that of pD = 10.9 (Fig. 6B).

Using density functional theory (DFT), the self-aggregation was simplified by considering dimers of caproleic acid and oleic acid in the neutral and anionic forms. Geometry optimizations and vibrational frequency calculations were carried out using Gaussian16⁸ with the ωB97X-D⁹ density functional, which incorporates long-range correction and empirical dispersion.

An augmented correlation-consistent basis set, the aug-cc-pVDZ, was employed to model the more diffuse characteristics of the atomic anion.¹⁰ Frequency calculations were performed to confirm that all optimized geometries were true minima. For each system, the two molecules were initially arranged in a parallel configuration, and the total energy was minimized to determine whether this approach results in stabilization. For caproleic acid, a dimer was analyzed with an implicit solvent model (IEFPCM using water as the dielectric medium),¹¹ starting from parallel structures, motivated by the NOE results. To reduce computational costs, the gas-phase optimized geometry of oleic acid was used as the initial guess for the subsequent re-optimization using the implicit solvation model. All reported structures and energies correspond to the final solvated minima. The results are presented in Fig. 7. For the caproleic acid dimer, the form of the carboxyl group produces a structure that deviates from parallelism (Fig. 7A and B) mainly due to the hydrogen bond formed between the carboxyl groups. In the anionic form, though, the parallelism is achieved primarily due to the hydrophobic effect (Fig. 7C and D).

For oleic acid in its ionic form, a stable configuration was identified where one molecule adopts a folded conformation around the alkyl tail of another molecule, stabilized by hydrophobic interactions between the aliphatic chains (Fig. 7E and F).



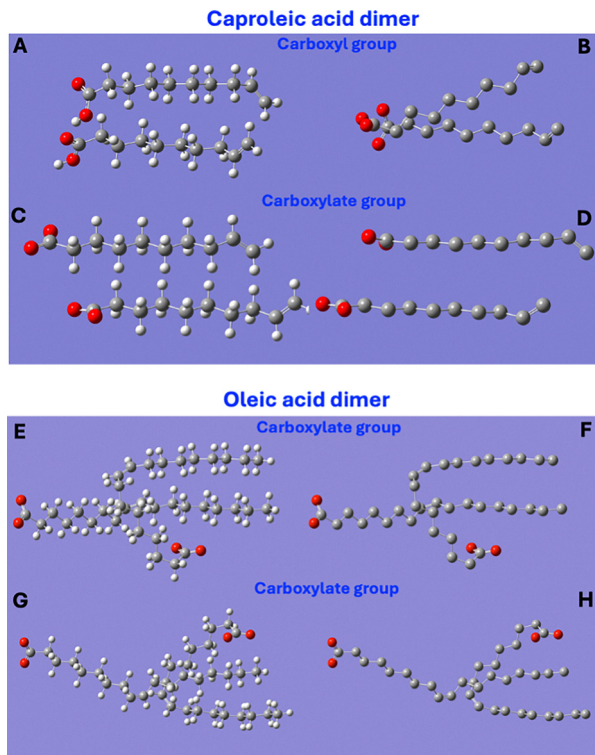


Fig. 7 Energy minimized structures of caproelic acid (A) and (B), caproelic acid anion (C) and (D), and oleic acid anion (E)–(H) in two different configurations at the ω -B97X-D level of theory with the aug-cc-pVDZ basis set using the IEFPCM implicit solvation model.¹¹

Motivated by the NOE data, we constructed an additional starting geometry in which the carboxylate group of one molecule was positioned to interact with the terminal methyl group of another. Geometry optimization of this setup produced a distinct, energetically minimized structure (Fig. 7G and H). Our calculations revealed a unique oleate dimer arrangement in which the carboxylate group approaches the terminal methyl of a second molecule (Fig. 7G and H), in excellent agreement with the NOE data. To our knowledge, such a carboxylate–methyl contact has not been explicitly reported in fatty acid dimers; related studies highlight head-to-head hydrogen bonding in neutral acids and mainly hydrophobic tail packing in carboxylates. Although $\text{CH} \cdots \text{O}$ interactions involving terminal methyl groups are inherently weak, their presence here supports the overall hydrophobic stabilization of the alkyl chains and shows a subtle geometric pattern consistent with the experimental data.

In summary, we have shown through the combined use of $^1\text{H}/^{13}\text{C}$ NMR and DFT calculations that the $\text{p}K_{\text{a}}$ values of caproelic acid and oleic acid in aqueous solution are not abnormally high and are within the $\text{p}K_{\text{a}}$ values of typical organic carboxylic acids.

This research was co-financed by the Hellenic Foundation for Research and Innovation (H.F.R.I.) under the “First Call for H.F.R.I. Research Projects to support faculty members and researchers and the procurement of high-cost research equipment grant” (project number 2050 to I. P. G.) and the Slovenian

Research and Innovation Agency (ARIS) (research grants J1-4400 and P1-0010 to S. G. G. and T. G.).

Conflicts of interest

There are no conflicts to declare.

Data availability

The data supporting this article have been included as part of the supplementary information (SI). Supplementary information: NMR experiments, DFT calculations, and Cartesians of optimized structures. See DOI: <https://doi.org/10.1039/d5cc05822h>.

Notes and references

- (a) D. E. Vance and J. E. Vance, *Biochemistry of lipids, lipoproteins and membranes (new comprehensive biochemistry)*, Elsevier, Amsterdam, Netherlands, 5th edn, 2008; (b) C. C. Akoh and D. B. Min *Food lipids, chemistry, nutrition and biochemistry*, Marcel Dekker Inc., New York, 2nd edn, 2002; (c) C. Leray *Dietary lipids for healthy brain function*, CRC Press, USA, 2021; (d) E. Alexandri, R. Ahmed, H. Siddiqui, M. I. Choudhary, C. G. Tsiafoulis and I. P. Gerotheranassis, *Molecules*, 2017, **22**, 1663.
- (a) O. Quehenberger and E. A. Dennis, *N. Engl. J. Med.*, 2011, **365**, 1812–1823; (b) P. Yli-Jama, H. E. Meyer, J. Ringstad and J. I. Pedersen, *J. Intern. Med.*, 2002, **251**, 19–28; (c) A. H. Huber and A. M. Kleinfeld, *J. Lipid Res.*, 2017, **58**, 578–585.
- (a) C. J. Porter, N. L. Trevaskis and W. N. Charman, *Nat. Rev. Drug Discovery*, 2007, **6**, 231; (b) M. J. Hackett, J. L. Zang, W.-C. Shen, P. C. Guley and M. J. Cho, *Adv. Drug Delivery Rev.*, 2013, **65**, 1331; (c) N. Fattahi, M.-A. Shahbazi, A. Maleki, M. Hamidi, A. Ramazani and H. A. Santos, *J. Controlled Release*, 2020, **326**, 556.
- W. Ma, B. Yang, H. Zhang and D. Sun, *J. Mol. Liq.*, 2023, **390**, 123133.
- (a) T. H. Haines, *Proc. Natl. Acad. Sci. U. S. A.*, 1983, **80**, 160–164; (b) J. R. Kanicky, A. F. Poniatoski, N. R. Mehta and D. O. Shah, *Langmuir*, 2000, **16**, 172–177; (c) J. R. Kanicky and D. O. Shah, *Langmuir*, 2003, **19**, 2034–2038; (d) R. E. Heikkila, D. W. Deamer and D. G. Cornwel, *J. Lipid Res.*, 1970, **11**, 195; (e) R. A. Peters, *Proc. R. Soc. London, Ser. A*, 1931, **133**, 140; (f) A. P. Christodoulou and H. L. Rosano, *Adv. Chem. Ser.*, 1968, **84**, 210; (g) J. R. Kanicky and D. O. Shah, *J. Colloid Interface Sci.*, 2002, **256**, 201–207; (h) Y. D. Vysotsky, E. S. Kartashynska, D. Vollhardt and V. D. Fainerman, *J. Phys. Chem. C*, 2020, **124**, 13809.
- (a) M. A. Kenyon and J. A. Hamilton, *J. Lipid Res.*, 1994, **35**, 458–467; (b) I. Petipras, T. Grüne, A. A. Bhattacharya and S. Curry, *J. Mol. Biol.*, 2001, **314**, 955–960; (c) J. R. Simard, P. A. Zunszain, C.-E. Ha, J. S. Yang, N. V. Bhagavan, I. Petipras, S. Curry and J. A. Hamilton, *Proc. Natl. Acad. Sci. U. S. A.*, 2005, **102**, 17958–17963; (d) E. S. Krenzel, Z. Chen and J. A. Hamilton, *Biochemistry*, 2013, **52**, 1559–1567; (e) E. Alexandri, A. Primikyri, G. Papamokos, T. Venianakis, V. K. Gkalpinos, A. G. Tzakos, A. Karydis-Messinis, D. Moschovas, A. Avgeropoulos and I. P. Gerotheranassis, *FEBS J.*, 2022, **289**, 5617–5636; (f) E. Alexandri, T. Venianakis, A. Primikyri, G. Papamokos and I. P. Gerotheranassis, *Molecules*, 2023, **28**, 3724; (g) T. Venianakis, A. Primikyri, T. Opatz, S. Petry, G. Papamokos and I. P. Gerotheranassis, *Molecules*, 2023, **28**, 7991; (h) A. M. de Urquiza, S. Liu, M. Sjöberg, R. H. Zetterström, W. Griffiths, J. Sjövall and T. Perlman, *Science*, 2000, **290**, 2140–2144; (i) M. Rademacher, A. W. Zimmerman, H. Rüterjans, J. H. Veerkamp and C. Lücke, *Mol. Cell. Biochem.*, 2002, **239**, 61–68.
- R. Hagen and J. D. Roberts, *J. Am. Chem. Soc.*, 1969, **91**, 4504.
- M. J. Frisch *et al.*, *Gaussian 16 Rev. B.01*, Wallingford, CT, 2016.
- J. D. Chai and M. Head-Gordon, *J. Chem. Phys.*, 2008, **128**(8), 084106.
- T. H. Dunning, *J. Chem. Phys.*, 1989, **90**(2), 1007–1023.
- E. Cancès, B. Mennucci and J. Tomasi, *J. Chem. Phys.*, 1997, **107**, 3032–3041.

